Metals and Materials International (2019) 25:1593–1602
https://doi.org/10.1007/s12540-019-00301-7

Hollow Twist Extrusion: Introduction, Strain Distribution, and Process Parameters Investigation

J. Joudaki[1] · M. Safari[1] · S. M. Alhosseini[1]

Received: 27 February 2019 / Accepted: 14 May 2019 / Published online: 28 May 2019

Abstract

Twist Extrusion is kind of severe plastic deformation process which enhances the strength of materials by applying a shear plastic strain and consequently grain refinement. The strain distribution is minimum at the center of the die and is maximum at outer surfaces. In this article, the plastic strain distribution will be studied within a hollow section. The billet is solid in previous experimental and numerical studies in the literature, but by adding a new die (mandrel) for extruding the hollow billet, it is possible to twist extrude hollow sections. A finite element model is developed in the ABAQUS finite element software and the effects of process parameters (slope line angle, thickness and friction coefficient) on equivalent plastic strain distribution are investigated. The numerical results show that the equivalent plastic strain will be increased by increasing the slope line angle and decreasing the thickness and more homogeneity in the strain field will be obtained. In addition, increasing the friction coefficient higher than 0.2 can lead to an increase in induced plastic strain. The required force for twist extrusion will be increased by increasing the friction coefficient.

Graphical Abstract

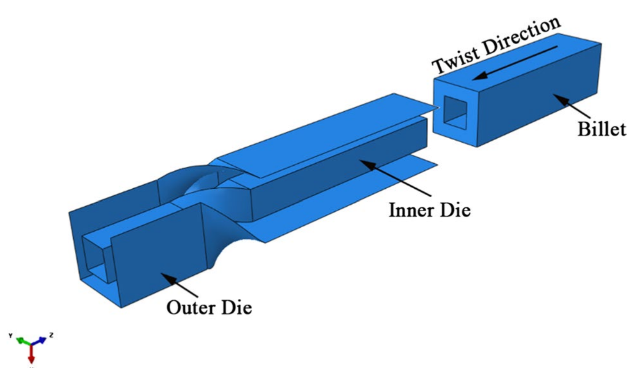

Keywords Hollow twist extrusion · HTE · Strain distribution · Slope line angle · Hollow section

1 Introduction

In recent years, different new severe plastic deformation (SPD) techniques are introduced to produce bulk ultrafine grain (UFG) materials. Some of the methods are in the category of top-down, which refines the grains of bulk material and produce nanosize grains. The introduced methods have corresponding stress and strain distribution, but non-uniform plastic strain distribution can be observed in many of them. The hardening of the sample depends on grain

✉ J. Joudaki
joudaki@arakut.ac.ir

[1] Department of Mechanical Engineering, Arak University of Technology, Daneshgah Street, PO Box 41167-38181, Arak, Iran

refinement and work hardening at low temperature, So, the SPD processes are done as cold processes. The obtained microstructures are in the range of sub-micron, and in some cases, nanoscales (~100 to 300 nm) [1, 2]. Main advantages of the SPD process are the higher strength and relatively appropriate formability which makes the UFG materials superior to others [3–5]. The size of the workpiece is almost remaining unchanged after performing the process and the process can be repeated in different passes to accumulate the induced plastic strain distribution and obtain more homogeneous strain distribution in the sample [6, 7]. In most SPD processes, the maximum increase in the yield strength and ultimate tensile strength happens at the first pass of the process [8]. Different SPD processes are developed by the researchers, the most famous SPD processes are equal channel angular pressing (ECAP) and equal channel angular rolling (ECAR) [9–11], high-pressure torsion (HPT) [12, 13], and twist extrusion (TE) [14–18]. In the beginning, the TE process introduced and developed by Beygelzimer et al. [19–21].

The die of TE consists of upper and lower straight channels and a twisting channel in the middle. The cross-section of the inlet and outlet are equal but the twist section forces the sample to twist and a shear strain will be created in the plane strain section, consequently, the grain refinement and material deformation will happen in the middle zone of the die (material deformation zone) [19]. Figure 1 shows a schematic illustration of a twist extrusion process. The material deformation zone or twisting zone can be represented by a slope line angle and rotation angle. The main difference of TE with other SPD process is the existence of two shear planes in the die (at the entrance and exit of the twisting channel), So, higher strain values can be obtained at outer surfaces of the sample compared to other SPD processes, such as ECAP [17]. However, the strain distribution is not homogenous and varies from the center of the sample to the outer surfaces of the sample.

Most of the developed SPD processes are in the laboratory scale and the industries did not use them conventionally.

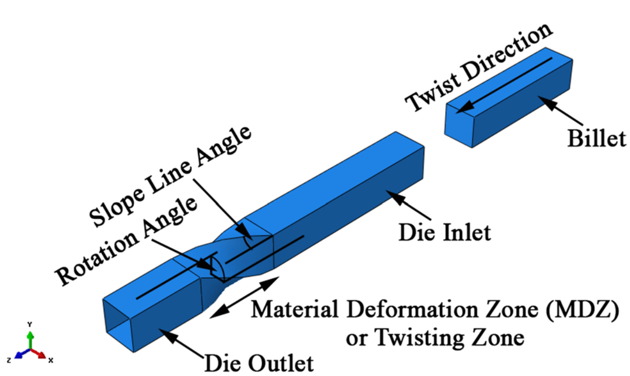

Fig. 1 Schematic illustration of twist extrusion (TE) process

The costing tool is the main concern. Nevertheless, several efforts have been done to investigate different aspects of SPD processes and their effects on different materials [22–24]. Several pieces of research are published to emphasize the effect of process parameters [22–31]. Twist extruding of elliptical cross-section [25], effect of the material [23, 26], spiral equal channel angular extrusion [27], planar twist extrusion [28], off-axis twist extrusion [29], tubular channel angular pressing [31] and multi-channel spiral twist extrusion (MCSTE) [32] are examples of researches developed based on twist extrusion. In addition, modification and combination of two different SPD processes for example ECAP and TE are also interesting [22, 25, 33]. Professor Yan Beygelzimer is one of the outstanding researchers who published several pieces of research in the TE. Recently a review article was published by Beygelzimer et al. [34] and an extensive survey of the literature on the mechanics of TE was published. The effect of twist extrusion on the microstructural evolution, mechanical properties, behavior of different materials during TE and the material flow during TE was discussed.

As it was mentioned in the literature until now, all of the researches have been focused on the twist extrusion process of solid specimens. To the authors' knowledge, there is not any research on the hollow twist extrusion process. Though, in this article, the hollow twist extrusion process will be introduced and will be investigated using the finite element analysis by ABAQUS software. For this purpose, the effects of process parameters such as slope line angle, thickness and friction coefficient on the equivalent plastic strain distribution will be probed.

2 Finite Element Modeling

The twist extrusion consists of extruding a billet through a die. Therefore, a finite element model has been developed in the ABAQUS software. It is supposed that the billet was made from AA-1050 aluminum alloy. The material properties of billet were extracted from [33]. The elastic modulus and Poisson's ratio are defined as 70 GPa and 0.33 respectively. The billet is a hollow square with 30 mm × 30 mm external dimensions. The internal square hole is different. The cross sections of the initial billet are adjusted as 15 mm × 15 mm while studying the effect of slope line angle and friction coefficient. However, for investigation of thickness, the cross section is additionally changed to 18.75 mm × 18.75 mm, 22.5 mm × 22.5 mm and 26.25 mm × 26.25 mm. The length of the initial billet is also 100 mm. Fig. 2 shows the billet and dies in the isometric view. Three faces of the outer die are set as hidden to better view the inner die. The cross sections of TE die are considered appropriate with the initial billet dimensions.

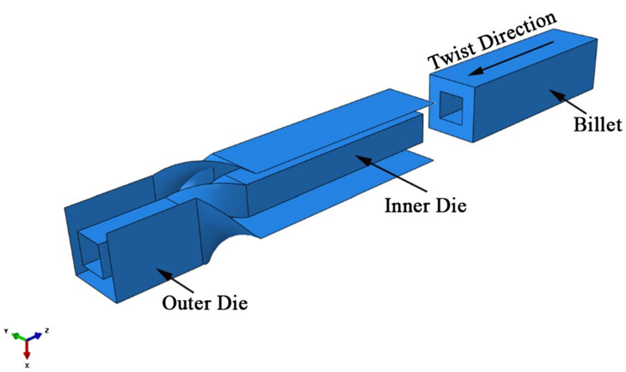

Fig. 2 Schematic illustration of the hollow twist extrusion dies and the initial billet

Table 1 Length of twist section for different slope line angle

Slope line angle	Length of twist section (mm)
30	51.9615
45	30
60	17.3205

A concentric mandrel similar to outer die is placed at the center. The die was modeled as a rigid part. The rotation angle is 90° clockwise and the length of the twisting section defined as Table 1.

The finite element analysis was done by the explicit solver of the software with enabled nonlinear geometry. The surface-to-surface contact was selected to define the contact between the billet and the die surfaces. The billet was forced to move 100 mm downward to quit the billet from the die. This billet is meshed by a 3D, 8-node brick continuum element with reduced integration calculation (C3D8R). The die was meshed by a 4-node 3D bilinear rigid quadrilateral element (R3D4). A mesh sensitivity analysis was carried out and 1 mm mesh size was selected for simulation. Table 2 shows the selected process parameters includes slope line angle, thickness and friction coefficient for numerical investigations. It should be noted that the main analysis was done with slope line angle 45°, 7.5 mm thickness and 0.1 friction coefficient. The other variations are implemented according to the One Factor At Time (OFAT) procedure in the design of experiments method. The literature review shows that higher slope line angles led to more deformation and induced strain.

3 Results and Discussion

3.1 Verification of the FE Model

As described in the Introduction section, the twist extrusion process is done only for the full solid section and this article is introducing a hollow twist extrusion concept. In this way, for verification of the finite element model, the finite element model was modified to extrude a section similar to Kim et al. [33]. The article extrudes a 10 mm × 10 mm square section by 45° slope line angle of the die from AA1050 aluminum alloy. The material property and frictional condition were defined similarly to Kim et al. [33]. After completing the analysis, the results of the FE model are compared to the reported results of [33] (Fig. 3). The path of plotting the results is defined from the left edge to the right edge of the section (at the middle of width). Comparison of the results show good agreement between the FE model and reported results of Kim et al. [33]. The mesh size is not specified at Ref. [33] and part of the difference may be associated with the element size in the FE model.

Table 2 The process parameters variation in the finite element simulations

	Die slope line angle	Thickness of billet (mm)	Friction coefficient
Variation of slope line angle	30	7.5	0.1
	45		
	60		
Variation of thickness	45	7.5	0.1
		5.625	
		3.75	
		1.875	
Variation of friction coefficient	45	7.5	0 (no friction)
			0.1
			0.2
			0.3

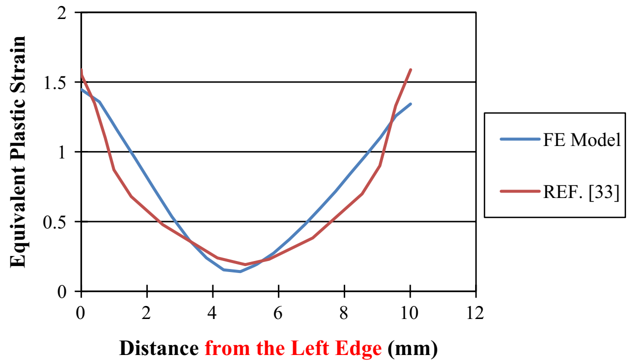

Fig. 3 Comparison of the equivalent plastic strain distribution for verification

3.2 Effect of Slope Line Angle

Figure 4 shows the Von Mises stress and equivalent plastic strain (PEEQ) distribution obtained by the finite element analysis of the twist extrusion process. A path is defined across the center of the hollow square section. Figure 5 shows the equivalent plastic strain (PEEQ) distribution along the defined path for different slope line angle. The horizontal dotted line corresponds to the hollow zone and it is not existing physically. The results show that a higher magnitude of plastic strain will be obtained by increasing the slope line angle. In addition, the inner surfaces of the section experience higher strains depending on the slope line angle.

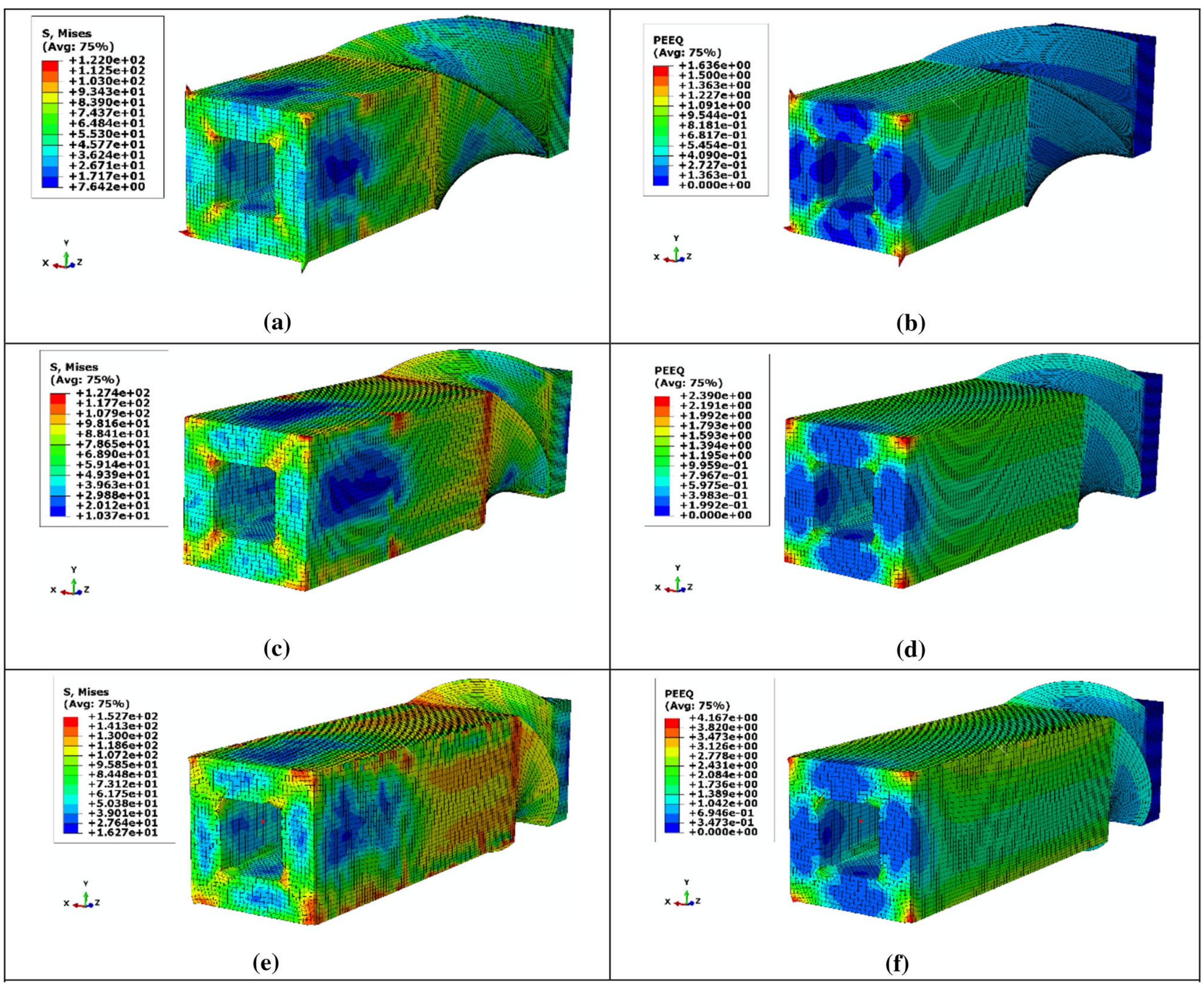

Fig. 4 The Von Mises stress and equivalent plastic strain distribution for slope line angle **a**, **b** 30°; **c**, **d** 45°; **e**, **f** 60°

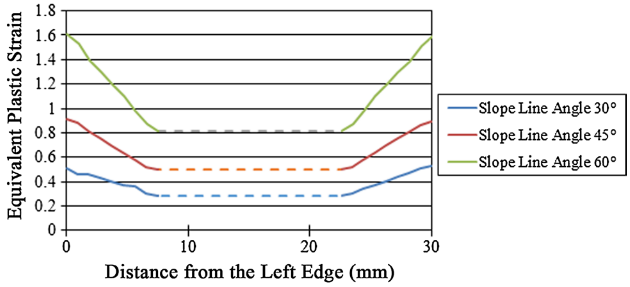

Fig. 5 Comparison of equivalent plastic strain distribution across the centerline of the section for different slope line angle

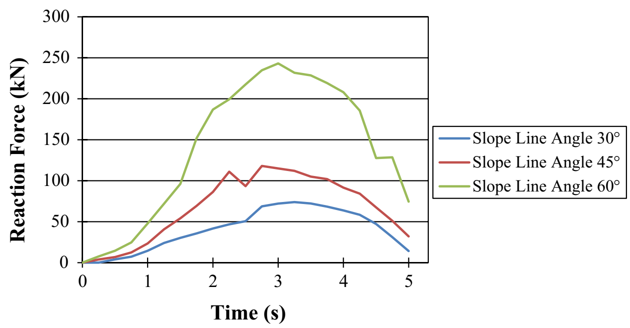

Fig. 6 Comparison of the required force for twist extruding of billet with different slope line angle

Figure 6 shows the required force for extruding different samples obtained from finite element analysis.

According to the results of Figs. 4, 5 and 6, increasing the slope line angle leads to higher residual stress distribution in the final billet. The magnitude of stress is higher at the corners of the billet, which experiences more plastic deformation. In addition, the maximum of plastic strain increases by increasing the slope line angle and it can be observed at the corners of billet. By increasing the slope line angle, the area of the region that has higher plastic strains will be decreased and in the slope line angle 60° become minimum. More homogeneity in plastic strain distribution can be observed for a higher slope line angle. This is due to the decrease in the length of the material deformation zone (MDZ) in the die and increasing the rate of deformation behavior in twist extruding. Consequently, the required force for extruding the billet through the die will be increased by increasing the slope line angle. The maximum force required for twist extruding are 73, 118 and 243 kN for 30°, 45° and 60° slope line angle. The required force increased by 61.6% and 232.8% compared to the 30° slope line angle.

3.3 Effect of Thickness

Figure 7 shows the distribution of Von Mises stress and equivalent plastic strain in hollow twist extrusion. The cross section is 30 mm × 30 mm. The results show that when the section is fully solid and no hole exists, a large area of the sample will experience very low plastic strains. Decreasing the thickness leads to more stress concentration at four corners of the extruded section, hence the maximum of stress (residual stress) will be increased. In addition, by decreasing the thickness more homogeneity in the stress will be seen and warping of corners increases at lower thickness. The corners have the highest plastic strain and consequently higher strength (flow stress). By decreasing the thickness, the maximum of residual plastic strain will be increased. The difference between the maximum and minimum plastic strains reduces by decreasing the thickness and more homogeneity in the strain distribution can be observed.

Figure 8 shows the equivalent plastic strain distribution along the width of the sample passing from the centerline of the section. The x-axis distance starts from the left edge and ends at the right edge of the section. The slope line angle is 45° and the graphs show that the maximum value of plastic strain increases by decreasing the thickness. Comparing the equivalent plastic distribution in Fig. 8 shows that the slope of the graphs for hollow sections is similar to the full solid section and in the zones which no material exists, the strain distribution does not exist. This is due to applying more pressure at the workpiece and increasing the role of shear stress induced by twisting. The horizontal dotted lines show the inner zone of the hollow section which no material exists in this zone. Comparing the results of plastic strain distribution in Fig. 7 and the plots of Fig. 8 demonstrate that higher values of plastic strain can be seen in the contours which are not presented in the plots. Figure 7 shows that maximum plastic strain value exists at the corners and minimum plastic strain value exists at the center of the lateral edges. The induced strains correspond to the distance from the center of the die. So, the difference between the maximum values of plastic strain in Figs. 7 and 8 relates to the location of graph plots in Fig. 8. The graphs of Fig. 8 are plotted at the middle of width crossing from the center. Figure 9 shows the variation of the required force for twist extrusion for different thicknesses. The required force of TE is almost equal for 5.625 mm, 3.75 mm and 7.5 mm (which is not shown in the figure for more clarity) in comparison by the required force for the full solid section. However, when thickness decreases to 1.875 mm, the required force will be increased considerably. This is due to increasing the contact between the workpiece and die and the resist of material against induced shear stress due to the twisting in the material deformation zone. By decreasing the thickness, the area of the inside square hole will be increased, consequently, the friction force of the internal surface will be increased. The maximum of TE force is 108, 117 and 115 kN for the solid section, 5.625 mm, 3.75 mm thickness respectively. This force is 369 kN for 1.875 mm thickness which shows about

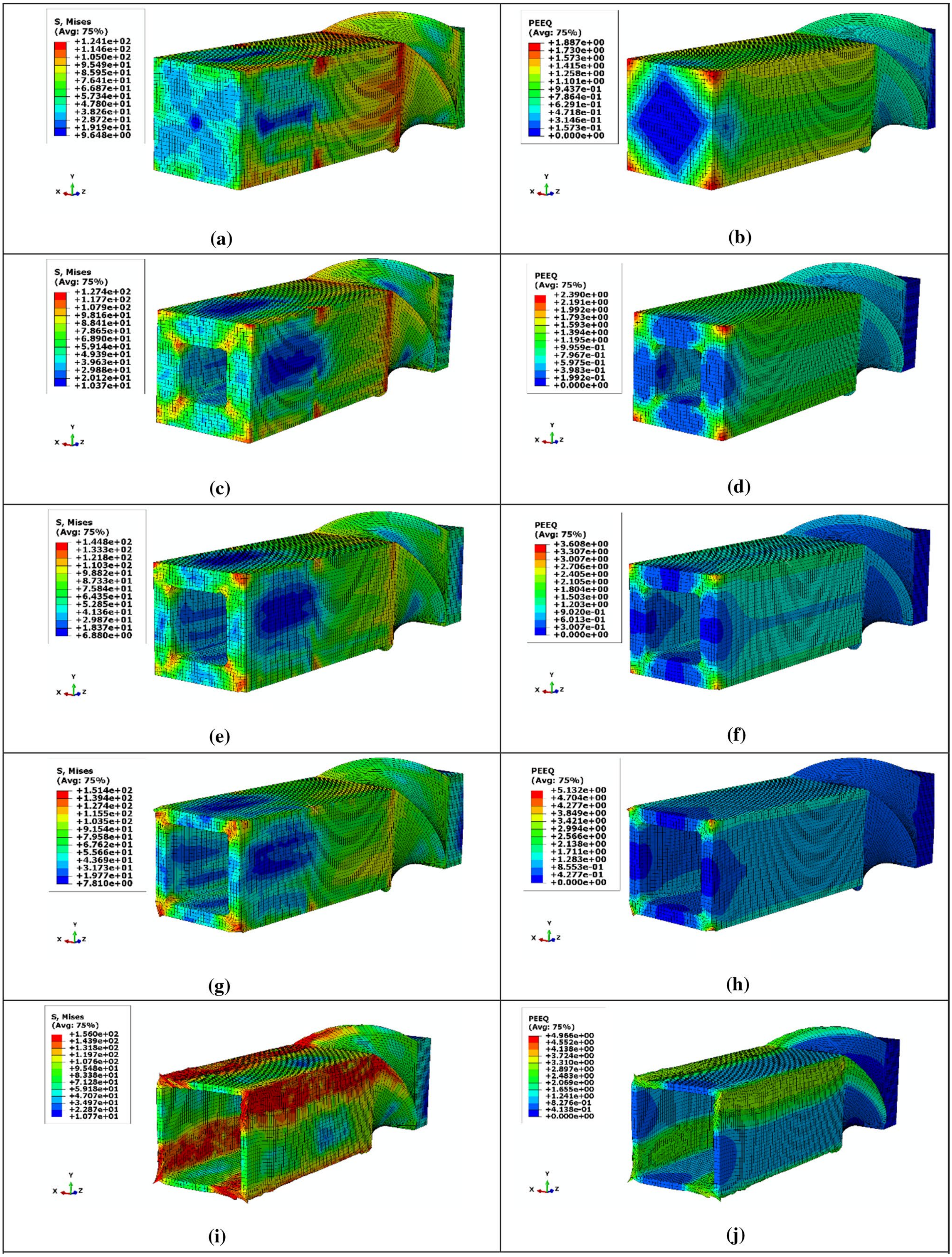
S, Mises
(Avg: 75%)
+1.241e+02
+1.146e+02
+1.050e+02
+9.549e+01
+8.595e+01
+7.641e+01
+6.687e+01
+5.734e+01
+4.780e+01
+3.826e+01
+2.872e+01
+1.919e+01
+9.648e+00
Y
X
Z
(a)
PEEQ
(Avg: 75%)
+1.887e+00
+1.730e+00
+1.573e+00
+1.415e+00
+1.258e+00
+1.101e+00
+9.437e-01
+7.864e-01
+6.291e-01
+4.718e-01
+3.146e-01
+1.573e-01
+0.000e+00
Y
X
Z
(b)
S, Mises
(Avg: 75%)
+1.274e+02
+1.177e+02
+1.079e+02
+9.816e+01
+8.841e+01
+7.865e+01
+6.890e+01
+5.914e+01
+4.939e+01
+3.963e+01
+2.988e+01
+2.012e+01
+1.037e+01
Y
X
Z
(c)
PEEQ
(Avg: 75%)
+2.390e+00
+2.191e+00
+1.992e+00
+1.793e+00
+1.593e+00
+1.394e+00
+1.195e+00
+9.959e-01
+7.967e-01
+5.975e-01
+3.983e-01
+1.992e-01
+0.000e+00
Y
X
Z
(d)
S, Mises
(Avg: 75%)
+1.448e+02
+1.333e+02
+1.218e+02
+1.103e+02
+9.882e+01
+8.733e+01
+7.584e+01
+6.435e+01
+5.285e+01
+4.136e+01
+2.987e+01
+1.837e+01
+6.880e+00
Y
X
Z
(e)
PEEQ
(Avg: 75%)
+3.608e+00
+3.307e+00
+3.007e+00
+2.706e+00
+2.405e+00
+2.105e+00
+1.804e+00
+1.503e+00
+1.203e+00
+9.020e-01
+6.013e-01
+3.007e-01
+0.000e+00
Y
X
Z
(f)
S, Mises
(Avg: 75%)
+1.514e+02
+1.394e+02
+1.274e+02
+1.155e+02
+1.035e+02
+9.154e+01
+7.958e+01
+6.762e+01
+5.566e+01
+4.369e+01
+3.173e+01
+1.977e+01
+7.810e+00
Y
X
Z
(g)
PEEQ
(Avg: 75%)
+5.132e+00
+4.704e+00
+4.277e+00
+3.849e+00
+3.421e+00
+2.994e+00
+2.566e+00
+2.138e+00
+1.711e+00
+1.283e+00
+8.553e-01
+4.277e-01
+0.000e+00
Y
X
Z
(h)
S, Mises
(Avg: 75%)
+1.560e+02
+1.439e+02
+1.318e+02
+1.197e+02
+1.076e+02
+9.548e+01
+8.338e+01
+7.128e+01
+5.918e+01
+4.707e+01
+3.497e+01
+2.287e+01
+1.077e+01
Y
X
Z
(i)
PEEQ
(Avg: 75%)
+4.966e+00
+4.552e+00
+4.138e+00
+3.724e+00
+3.310e+00
+2.897e+00
+2.483e+00
+2.069e+00
+1.655e+00
+1.241e+00
+8.276e-01
+4.138e-01
+0.000e+00
Y
X
Z
(j)

◂**Fig. 7** The Von Mises stress and equivalent plastic strain distribution for different thickness **a**, **b** solid section; **c**, **d** 7.5 mm; **e**, **f** 5.625 mm; **g**, **h** 3.75 mm; **i**, **j** 1.875 mm

a 220% increase in force. Therefore, the required force for extruding will be increased by decreasing the thickness to a very small value.

Figure 8 shows that the difference between the plastic strain distributions is small enough to neglect the changes (about 2% difference can be seen). The previous researches [5, 12] show that the minimum and maximum of the plastic strain can be described by Eqs. 1 and 2.

$$\varepsilon_{min} \approx a + btan\beta \tag{1}$$

$$\varepsilon_{max} \approx \frac{2}{\sqrt{3}}tan\beta \tag{2}$$

a and b are constant and β is the slope line angle. According to Fig. 8 and Eqs. 1 and 2, the equivalent plastic strain in the twist-extruded workpiece can be expressed by Eq. 3.

$$\varepsilon^p = \begin{cases} 0.04 + \frac{r}{\frac{\sqrt{2}}{2}a}tan\beta & -\frac{a}{2} \le r \le -\frac{a_i}{2} \\ No\ physical\ material & -\frac{a_i}{2} < r < \frac{a_i}{2} \\ 0.04 + \frac{r}{\frac{\sqrt{2}}{2}a}tan\beta & \frac{a_i}{2} \le r \le \frac{a}{2} \end{cases} \tag{3}$$

a_i and a are the internal out external width of the hollow square section and r is the radial distance from the center of the square. The constant number (0.04) stands for the cross-flow of material at the center of the die.

It should be noted that the material flow during twist extrusion consists of two parts: a helical flow and deviations from the helical flow. The helical flow is created due to the ideal twisting of the billet in the die. The helical flow varies according to the relative location from the center of twisting. The cross-flow is determined as deviations from the helical flow, resulting in planar flow within a virtual transverse section of the billet. In contrast to the ideal helical flow, the cross-flow leads to displacement of the material points from their initial locations in cross-section. Equation 3 shows the two mentioned material flow. Researches show that the cross flow increases by increasing the slope line angle and increasing the friction coefficient between the die and the billet [35]. When the cross-flow is weak, the cross-section of a solid billet rotates as a rigid body when the billet moves through the twisting channel. In this case, a velocity field for the twist extrusion of a hollow billet on a rigid mandrel practically coincides with a velocity field for the twist extrusion of a solid billet. The good agreement between the results of plastic strain distribution in the hollow section and solid section can be explained based on the material flow in the twist extrusion process.

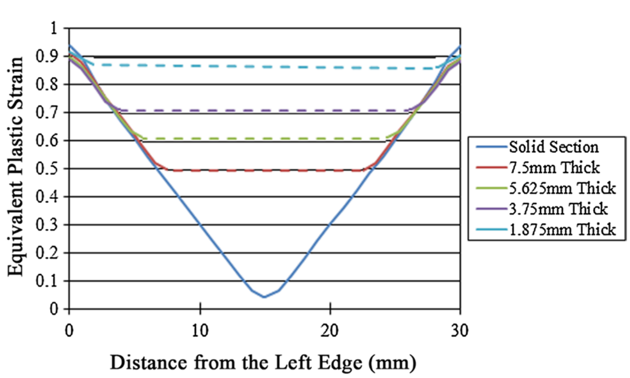

Fig. 8 Comparison of equivalent plastic strain distribution across the centerline of the section for different thickness

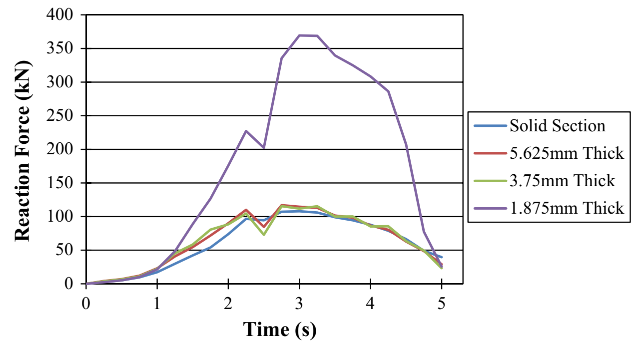

Fig. 9 Comparison of the required force for twist extruding of billet with different thickness

3.4 Effect of Friction Coefficient

Figure 10 shows the effect of the friction coefficient on Von Mises stress and equivalent plastic strain. Distribution of stress shows that the residual stress distribution is more uniform by increasing the friction coefficient. Moreover, the maximum stress at corners will be increased slightly. The elements distortion will be increased considerably by increasing the friction coefficient, which can be seen in Fig. 10g. Figure 11 shows the distribution of the equivalent plastic strain along the centerline of billet. Comparing the equivalent plastic strain in Figs. 11 and 10 it can be concluded that the strain distribution is almost constant at friction coefficient 0.1 and 0.2 and no friction. The magnitude of plastic strain at the contact surface will be increased slightly, but in the inner zone, the distribution is the same. However, the results for friction coefficient 0.3 is different and the strain distribution increased considerably. Furthermore, the

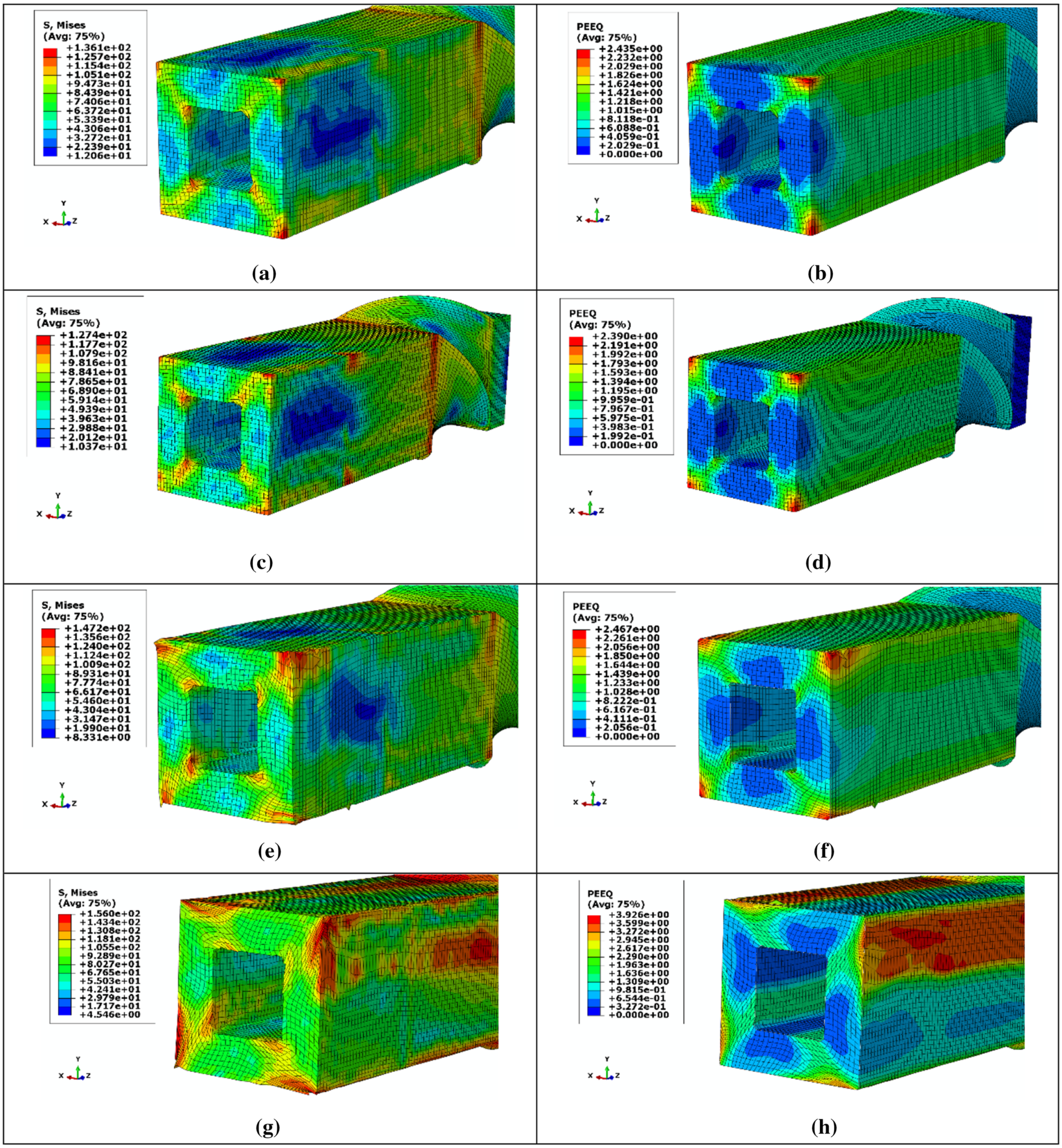

Fig. 10 The Von Mises stress and equivalent plastic strain distribution for different friction coefficient **a**, **b** no friction; **c**, **d** friction coefficient 0.1, **e**, **f** friction coefficient 0.2; **g**, **h** friction coefficient 0.3

small increase in the maximum value of plastic strain can be observed at the corners of the extruded billet. Figure 12 shows the required force for implementing the twist extrusion process with different friction coefficient. The required force will be increased by increasing the frictional force. The maximum force is considerably high for friction coefficient 0.3. So, increasing the friction coefficient more than 0.2 leads to consequently higher extruding force, more element distortion and higher plastic strain distribution.

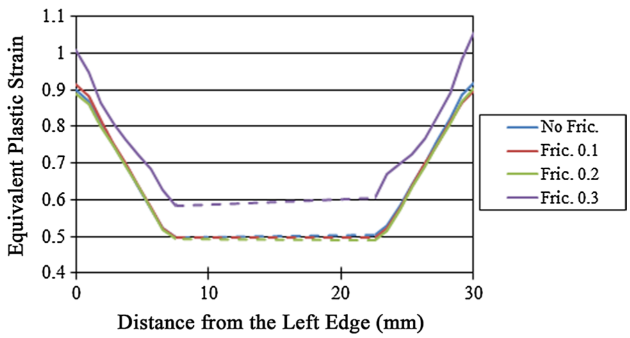

Fig. 11 Comparison of equivalent plastic strain distribution across the centerline of the section for different friction coefficient

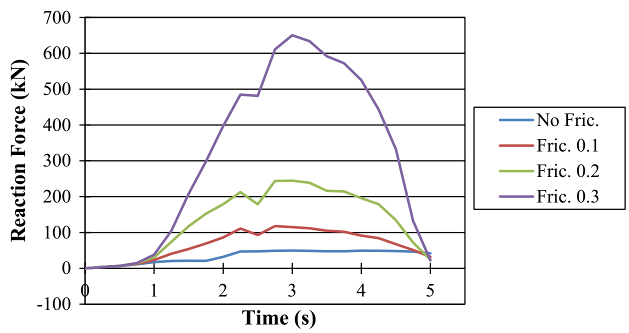

Fig. 12 Comparison of the required force for twist extruding of billet with different friction coefficient

4 Conclusions

In this article, a new setup for twist extruding of hollow sections were introduced and the effect of process parameters was investigated. The main outcome of this study can be emphasized as follows:

- The equivalent plastic strain distribution will be increased by increasing the slope line angle. The plastic strain at inner surfaces increases similar to outer surfaces.
- The required force for carrying out the twist extrusion will be increased by increasing the slope line angle.
- By decreasing the thickness, part of the section which has a low value of plastic strain will be eliminated and more uniformity in the plastic strain distribution will be obtained.
- The equivalent plastic strain distribution for different thicknesses are similar to plastic strain distribution of full solid section at a constant slope line angle.
- The required force of the twist extrusion will be increased for very small thicknesses.
- Low friction coefficient has a negligible effect on the plastic strain distribution, but the friction coefficient higher than 0.2 can lead to an increase in induced plastic strain due to twist extruding. The required force for twist extrusion will be increased by the friction coefficient.

In this article, the authors introduced a new configuration for hollow twist extrusion. The investigation has been done numerically. The next step in the development of the introduced process is the experimental tests and comparison of finite element results by the presented numerical results.

Compliance with Ethical Standards

Conflict of interest The authors declare that they have no conflict of interest.

References

1. J. Shen, V. Gärtnerová, L.J. Kecskes, K. Kondoh, A. Jäger, Q. Wei, Residual stress and its effect on the mechanical properties of Y-doped Mg alloy fabricated via back-pressure assisted equal channel angular pressing (ECAP-BP). Mater. Sci. Eng., A **669**, 110–117 (2016)
2. M. Sarkari Khorrami, M. Movahedi, Microstructure evolutions and mechanical properties of tubular aluminum produced by friction stir back extrusion. Mater. Des. **65**, 74–79 (2015)
3. B. Liu, Q. Lei, L. Xie, M. Wang, Z. Li, Microstructure and mechanical properties of high product of strength and elongation Al–Zn–Mg–Cu–Zr alloys fabricated by spray deposition. Mater. Des. **96**, 217–223 (2016)
4. R.Z. Valiev, T.G. Langdon, Principles of equal-channel angular pressing as a processing tool for grain refinement. Prog. Mater Sci. **51**, 881–981 (2006)
5. M. Ebrahimi, H. Gholipour, F. Djavanroodi, A study on the capability of equal channel forward extrusion process. Mater. Sci. Eng., A **650**, 1–7 (2016)
6. D.M. Jafarlou, E. Zalnezhad, M.A. Hassan, M.A. Ezazi, N.A. Mardi, A.M.S. Hamouda, M. Hamdi, G.H. Yoon, Severe plastic deformation of tubular AA 6061 via equal channel angular pressing. Mater. Des. **90**, 1124–1135 (2016)
7. M. Montazeri Pour, M.H. Parsa, H.R. Jafarian, S. Taieban, Microstructural and mechanical properties of AA1100 aluminum processed by multi-axial incremental forging and shearing. Mater. Sci. Eng., A **639**, 705–716 (2015)
8. M. Sedighi, P. Monshi, J. Joudaki, Investigation of mechanical properties and fatigue life of ECARed AA5083 aluminium alloy. Fatigue Fract. Eng. Mater. Struct. **40**, 412–422 (2017)
9. Y. Duan, L. Tang, G. Xu, Y. Deng, Z. Yin, Microstructure and mechanical properties of 7005 aluminum processed by room temperature ECAP and subsequent annealing. J. Alloys Compd. **664**, 518–529 (2016)
10. B. Leszcztnska-Madej, M.W. Richert, M. Perek-Nowa, Effect of severe plastic deformation on microstructure evolution of pure aluminum. Arch. Metall. Mater. **60**, 1437–1440 (2015)
11. A. Nassef, S. Samy, W.H. El-Garaihy, Enhancement of mechanical properties for Al–Mg–Si alloy using equal channel angular pressing. Int. J. Chem. Nucl. Mater. Metall. Eng. **9**, 131–136 (2015)

12. H.J. Lee, J.K. Han, S. Janakiraman, B. Ahn, M. Kawasaki, T. Langdon, Significance of grain refinement on microstructure and mechanical properties of an Al–3%Mg alloy processed by high-pressure torsion. J. Alloys Compd. **686**, 998–1007 (2016)
13. M. Murashkin, I. Sabirov, D. Prosvirnin, I. Ovid'ko, V. Terentiev, R. Valiev, S. Dobatkin, Fatigue behavior of an ultrafine-grained Al–Mg–Si alloy processed by high-pressure torsion. Metals **5**, 578–590 (2015)
14. D. Orlov, Y. Beygelzimer, S. Synkov, V. Varyukhin, N. Tsuji, Z. Horita, Microstructure evolution in pure Al processed with twist extrusion. Mater. Trans. **50**, 96–100 (2009)
15. U.M. Iqbal, V.S. Kumar, An analysis on effect of multi-pass twist extrusion process of AA6061 alloy. Mater. Des. **50**, 946–953 (2013)
16. Y. Beygelzimer, A. Reshetov, S. Synkov, O. Prokofevea, R. Kulagin, Kinematics of metal flow during twist extrusion investigated with a new experimental method. J. Mater. Process. Technol. **209**, 3650–3656 (2009)
17. S.R. Bahadori, S.A. Mousavi, A.R. Shahab, Investigation and numerical analysis of strain distribution in the twist extrusion of pure aluminum. JOM **63**, 69–76 (2011)
18. D. Orlov, Y. Beygelzimer, S. Synkov, V. Varyukhin, Z. Horita, Evolution of microstructure and hardness in pure al by twist extrusion. Mater. Trans. **49**, 2–6 (2008)
19. Y. Beygelzimer, V. Varyukhin, D. Orlov, S. Synkov, *Twist Extrusion Process for Strain Accumulation* (TEAN, Donetsk, 2003)
20. Y. Beygelzimer, Grain refinement versus voids accumulation during severe plastic deformations of polycrystals: mathematical simulation. Mech. Mater. **37**(2005), 753–767 (2005)
21. Y. Beygelzimer, V. Varyukhin, S. Synkov, D. Orlov, Useful properties of twist extrusion. Mater. Sci. Eng., A **503**, 14–17 (2009)
22. M.I. Latypov, E. Yoon, D. Lee, R. Kulagin, Y. Beygelzimer, M. Salehi, H. Kim, Microstructure and mechanical properties of copper processed by twist extrusion with a reduced twist-line slope. Metall. Mater. Trans. A **45**, 2232–2241 (2014)
23. D. Orlov, Y. Beygelzimer, S. Synkov, V. Varyukhin, N. Tsuji, Z. Horita, Plastic flow, structure and mechanical properties in pure Al deformed by twist extrusion. Mater. Sci. Eng., A **519**, 105–111 (2009)
24. S.A.A. AkbariMousavi, A.R. Shahab, M. Mastoori, Computational study of Ti–6Al–4V flow behaviors during the twist extrusion process. Mater. Des. **29**, 1316–1329 (2008)
25. M.I. Latypov, Y. Beygelzimer, H.S. Kim, Comparative analysis of two twist-based SPD processes: elliptical cross-section spiral twist extrusion vs. twist extrusion. Mater. Trans. **54**, 1587–1591 (2013)
26. M. Shamsborhan, M. Ebrahimi, Production of nanostructure copper by planar twist channel angular extrusion process. J. Alloys Compd. **682**, 552–556 (2016)
27. A. Fadaei, F. Farahafshan, S.S. Boroujeni, Spiral equal channel angular extrusion (Sp-ECAE) as a modified ECAE process. Mater. Des. **113**, 361–368 (2017)
28. Y. Beygelzimer, D. Prilepo, R. Kulagin, V. Grishaev, O. Abramova, V. Varyukhin, M. Kulakov, Planar twist extrusion versus twist extrusion. J. Mater. Process. Technol. **211**, 522–529 (2011)
29. Y. Beygelzimer, R. Kulagin, M.I. Latypov, V. Varyukhin, H.S. Kim, Off-axis twist extrusion for uniform processing of round bars. Metals Mater. Int. **21**, 734–740 (2015)
30. P. Frint, M. Hartel, R. Selbmann, D. Dietrich, M. Bergmann, T. Lampke, D. Landgrebe, M. Wagner, Microstructural evolution in metals subjected to simple shear by a particular severe plastic deformation method. Metals **8**, 1–13 (2018)
31. G. Faraji, M.M. Mashhadi, H.S. Kim, Tubular channel angular pressing (TCAP) as a novel severe plastic deformation method for cylindrical tubes. Mater. Lett. **65**, 3009–3012 (2011)
32. W.H. El-Garaihy, D.M. Fouad, H.G. Salem, Multi-channel spiral twist extrusion (MCSTE): a novel severe plastic deformation technique for grain refinement. Metall. Mater. Trans. A **49**, 2854–2864 (2018). https://doi.org/10.1007/s11661-018-4621-4
33. J.G. Kim, M. Latypov, N. Pardis, Y.E. Beygelzimer, H.S. Kim, Finite element analysis of the plastic deformation in tandem process of simple shear extrusion and twist extrusion. Mater. Des. **83**, 858–865 (2015)
34. Y. Beygelzimer, R. Kulagin, Y. Estrin, L.S. Toth, H.S. Kim, M.I. Latypov, Twist extrusion as a potent tool for obtaining advanced engineering materials: a review. Adv. Eng. Mater. **19**, 1600873 (2017). https://doi.org/10.1002/adem.201600873
35. R. Kulagin, M.I. Latypov, H.S. Kim, V. Varyukhin, Y. Beygelzimer, Cross flow during twist extrusion: theory, experiment, and application. Metall. Mater. Trans. A **44**, 3211–3220 (2013)